Available online at www.sciencedirect.com
ScienceDirect
Biosensors and Bioelectronics 23 (2008) 1259–1265
BIOSENSORS & BIOELECTRONICS
www.elsevier.com/locate/bios

Novel quartz crystal microbalance based biosensor for detection of oral epithelial cell–microparticle interaction in real-time

Jacqueline Elsom [a,*], Michael I. Lethem [a], Gareth D. Rees [b], A. Christy Hunter [a]

[a] *School of Pharmacy, University of Brighton, Lewes Road, Brighton BN2 4GJ, UK*
[b] *GlaxoSmithKline R&D, St. George's Avenue, Weybridge, Surrey KT13 0DE, UK*

Received 29 June 2007; received in revised form 24 October 2007; accepted 21 November 2007
Available online 22 January 2008

Abstract

Recent applications of quartz crystal resonant sensor technology to monitor cell adhesion and specific ligand interaction processes has triggered the development of a new category of quartz crystal microbalance (QCM) based biosensors. In this study human oral epithelial cells (H376) were cultured on quartz sensors and their response to microspheres investigated *in situ* using the QCM technique. The results demonstrated that this novel biosensor was able to follow cell–microsphere interactions in real-time and under conditions of flow as would occur in the oral cavity. Unique frequency profiles generated in response to the microspheres were postulated to be due to phases of mass addition and altered cellular rigidity. Supporting microscopic evidence demonstrated that the unique frequency responses obtained to these interactions were in part due to binding between the cell surface and the microspheres. Furthermore, a cellular uptake process, in response to microsphere loading was identified and this, by influencing the rigidity of the cellular cytoskeleton, was also detectable through the frequency responses obtained.

Keywords: Quartz crystal microbalance; Biosensor; Oral epithelial cells; Cell culture; Real-time

1. Introduction

The efficacy of conventional dosage forms employed to enhance oral hygiene is limited by the rapid decline in the concentration of actives after administration. Strategies to improve retention of pharmacological actives within the oral cavity have included the incorporation of bioadhesives and a number of methods exist to evaluate the ability of such compounds to interact with oral mucosal substrates for prolonged periods (Chickering and Mathiowitz, 1995 and Kockisch et al., 2003). Studies more pertinent to human oral epithelial cell behaviour include the use of buccal cell isolates (Kockisch et al., 2001) and cultured cells (Doucet et al., 1996; Lawrence. et al., 1996). Few studies currently allow dynamic assessment of such interactions under conditions of flow as would occur in the oral cavity (Farokhzad et al., 2005) and none currently utilise human oral epithelium under these conditions.

The quartz crystal microbalance (QCM) was originally developed to follow molecular adsorption at the gas–solid interface after Sauerbrey (1959) identified the existence of a linear relationship between mass addition at the piezoelectric substrate surface and change in the recorded resonant frequency. Development of the technique to monitor events in the liquid phase resulted in the application of the technique to a number of processes pertinent to biological research such as ligand–receptor interactions (Janshoff et al., 1997) characterisation of protein adsorption (Höök et al., 1998), nucleic acid hybridisation (Furtado and Thompson, 1998) and QCM based immunoassay (Aizawa et al., 2001).

The QCM technique is particularly attractive to the field of cell biology as it has the potential to monitor cell–surface interactions in a dynamic and non-invasive way. Thus it allows the generation of kinetic data, and as cumbersome labelling techniques are negated, the investigation of cellular responses without compromise to cellular architecture or protein structure. Such advantages have resulted in several pioneering studies which demonstrate the ability of the technique to monitor the adhesion and proliferation of a number of mammalian cell types *in situ* on the QCM surface (Matsuda et al., 1992; Redepenning et al., 1993; Gryte et al., 1993; Janshoff et al., 1996; Wegener et al., 1998, 2000). These preliminary studies identified that only specific, integrin-mediated cell-adhesion is detectable at the sensor

* Corresponding author. Tel.: +44 1273 642041; fax: +44 1273 679333.
E-mail address: J.Elsom@brighton.ac.uk (J. Elsom).

0956-5663/$ – see front matter © 2007 Elsevier B.V. All rights reserved.
doi:10.1016/j.bios.2007.11.020

surface. Furthermore, exploitation of this phenomenon revealed that the technique was sufficiently sensitive to discriminate between various substrates (as crystal surface modifications) and their impact on the cell adhesion process (Fredriksson et al., 1998a,b; Nimeri et al., 1998; Wegener et al., 2001; Cavic et al., 2001) resulting in the adoption of QCM technology as a routine tool in the field of biomaterials (Lord et al., 2006), and microbial biofilm research (Reipa et al., 2006).

Recent studies have demonstrated that the technique can detect cellular responses to chemical or biological stimuli as mediated through alterations in the cells' cytoskeletal architecture (Zhou et al., 2000; Cans et al., 2001; Marx et al., 2001, 2003). These studies highlight the potential to incorporate viable cells as signal transduction elements in combination with acoustic signal detection to investigate dynamic cellular responses to environmental modifications. To date, no studies have exploited these sensitive capabilities to investigate the response of oral keratinocytes to model microparticles that may ultimately be utilised in oral formulations, under conditions of flow as would occur in the oral cavity. Thus, the aims of this study were to develop a biosensor that incorporated a viable monolayer of human oral keratinocytes *in situ* on the quartz crystal surface to investigate cellular response to model microparticles, as might be used in oral healthcare formulations.

2. Experimental

2.1. Instrumentation

The QCM device was based on a novel surface mounted oscillation circuit with automatic gain control (AGC) designed to give extremely high amplitude oscillation with low noise, under liquid loading (Paul et al., 2001; Pavey et al., 2003). Gold-coated (100 nm thickness) 10 MHz AT-cut quartz crystals (8.6 mm diameter) were supplied with customised electrode configurations to allow both electrode contacts to be made on the crystal underside (Spartan Europe, UK). Crystals were mounted within a specially designed flow-cell and connected via flexible shielded electrodes to the oscillator head unit. Crystal oscillation data were recorded at 1 s intervals using a Fluka PM6685 frequency counter, connected via a PCIIa GPIB card to a personal computer (PC) running Fluka Timeview™ data acquisition and control software. The crystal oscillator and flow cell were housed in a thermostatically controlled oven set to 37 ± 0.1 °C (Denley, UK), and ambient and flow cell temperatures monitored using a 5-channel data logging electronic thermometer (PICOlog), K-type thermocouples (Radio Spares,UK) and dedicated software running on a second PC. Liquid delivery to the crystal surface (2–10 μL/min) was via PEEK® HPLC tubing using a Harvard syringe driver and glass gas-tight syringes (SGE Europe, UK). Samples were added to this mobile phase via a Rheodyne 9725 MBB™ HPLC injection valve fitted with a 20 μL PEEK® injection loop.

2.2. Cell culture

The oral epithelial cell line, H376, derived from a human squamous cell carcinoma (Prime et al., 1990) was employed throughout. Cells were cultured at 37 °C and 5% (v/v) CO_2 in Dulbecco's modified Eagle's medium (DMEM)/Hams F12 nutrient mix with 1 g/L glucose (Sigma–Aldrich, UK) supplemented with 10% (v/v) heat-inactivated foetal calf serum, 20 mM L-glutamine, 0.5 μg/mL hydrocortisone (Sigma–Aldrich, UK) and 2500 IU/mL penicillin and streptomycin (Invitrogen, UK). The culture media was exchanged on the first day after passage and then every 2 days thereafter. Routine subculturing of confluent cell layers was performed using standard trypsinisation (0.05% (w/v)/1.5 mM EDTA) after which the cells were seeded into fresh flasks at a density of 3×10^3 cells/cm^2. The cells were maintained in culture for no longer than ten passages during all experimental work to ensure that the neoplastic phenotype did not change as a result of prolonged passage *in vitro*.

2.3. Preparation of biosensors

Quartz crystals were cleaned by immersion in ethanol, spin-coated with polystyrene (0.5% w/v in toluene) as previously described (Fredriksson et al., 1998a) and treated in an oxygen-plasma for 2 min. This was shown to provide a suitably hydrophilic surface (receding water contact angle of less than 5°) designed to mimic that of tissue culture plastic and thus promote cell adhesion. Suspensions of H376 cells were prepared from near confluent monolayers using standard trypsinisation, 0.05% (w/v) trypsin/1.5 mM EDTA for 10 min at 37 °C. Petri dishes containing prepared crystals after their sterilisation by immersion into 70% ethanol were inoculated with cells at a density of 6×10^3 cells/cm^2. Control sensors to investigate frequency responses in the absence of cells were prepared by incubating modified quartz crystals in complete culture medium only.

2.4. Biosensor/microsphere interaction assay

DMEM/F12 nutrient mix with 15 mM HEPES (Sigma–Aldrich, UK) was equilibrated overnight at 37 °C and 5% (v/v) CO_2, syringe filtered (0.2 μm pore, Nunc) into a glass gas-tight syringe and used as the mobile phase. Biosensors were removed from cell culture on day 5 after cell seeding (the time taken to establish confluent monolayer coverage across the sensor surface) and installed within the flow cell. After connection to the oscillator circuit, the frequency response was monitored until a stable frequency baseline was established for the sensor under liquid loaded conditions (flow rate 5 μL/min). Fluorescent polystyrene microspheres (0.5 μm, Duke Scientific, Brookhaven International, UK) were diluted (0.05%w/v) in media and introduced to the mobile phase via the Rheodyne™ injection loop. The biosensor frequency response to the microspheres was monitored at 1 s intervals for 30 min. For each assay biosensors were prepared in triplicate to allow for comparison of cell viability between control sensors and those exposed to shear-wave excitation/serum depletion during the time course of experiments. Cell-free sensors were also used as controls to investigate the frequency response of the system to microsphere interactions in the absence of viscoelastic contribution from the cellular monolayer.

2.5. Cell viability assay

At the conclusion of oscillation experiments biosensors were removed from the flow-cell and cell viability evaluated using the method of Simm et al. (1997). Biosensors were incubated with propidium iodide (PI) and Hoechst 33342 (20 μg/mL final concentration in media) at 37 °C and 5% (v/v) CO_2 for 5 min. They were then examined using a broadband fluorescence filter set with excitation and emission wavelengths of λ365 and 397 nm respectively. Representative micrographs (20 fields) were taken from samples and controls (magnification× 320) and the numbers of viable, non-viable, apoptotic and necrotic cells were recorded using a semi-automated colony counter. These values were expressed as percentages of the total cell count and comparisons between samples and controls were determined using ANOVA.

2.6. Transmission electron microscopy

Cells grown on Thermanox® coverslips (Agar Scientific, UK) were fixed in glutaraldehyde (5% v/v in sodium cacodylate buffer, 0.05 M, pH 7.2) for 1 h at room temperature. The cells were then post-fixed in aqueous osmium tetroxide (2% v/v in sodium cacodylate) overnight at 4 °C and then rinsed in distilled water and pre-stained in aqueous uranyl acetate (0.5 v/v%) before dehydration through a graded alcohol series. Samples were embedded in Spurr resin (Agar Scientific, UK) and ultrathin sections (100 nm) prepared. Sections were post-stained with lead citrate and examined using a Phillips CM10 transmission electron microscope. Cells were also examined at the conclusion of biosensor experiments following processing after their removal from the sensor surface by trypsinisation.

2.7. Scanning electron microscopy

Prepared biosensors were incubated with polystyrene microsphere suspensions (0.05% w/v) in DMEM/F12 at 37 °C and 5% (v/v) CO_2 for 30 min and then processed for scanning electron microscopy (SEM) using a modified method of Norton et al. (1995). Samples were fixed in glutaraldehyde (5% v/v in sodium cacodylate buffer, 0.05 M, pH 7.2) for 1 h at room temperature (25 °C), washed in cacodylate/HCl buffer (0.05 M, pH 7.2) thrice and dehydrated through a graded ethanol series. Finally sensors were freeze dried (Christ T, Germany) for 2 h and then sputter coated with palladium (Polaron, UK) prior to examination using a JEOL 6310 scanning electron microscope at an accelerating voltage of 5 KeV.

3. Results and discussion

3.1. Control sensor/microsphere interaction assay

The interaction of microspheres with cell-free sensors served as a control to investigate frequency responses in the absence of any viscoelastic contribution from a cellular monolayer. Fig. 1 shows that each addition of microsphere suspension to the cell-free crystal surface resulted in a characteristic, time-dependent

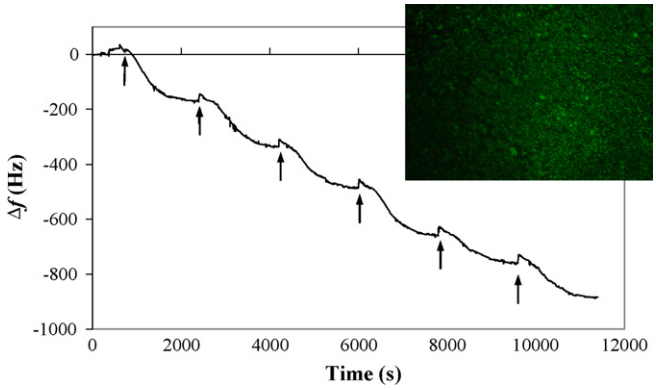

Fig. 1. Characteristic frequency response of a cell-free crystal to additions of microspheres (arrows indicate the time points at which injections were made). This demonstrates the frequency binding profile obtained in the absence of the viscoelastic cell layer and the continued responsiveness of the sensor to repeated microsphere additions. Inset: representative photomicrograph of the crystal surface at the conclusion of experiments to confirm the presence of the microspheres (Magnification× 200).

frequency decrease ($\Delta f_{binding}$) which lasted for approximately 1200 s, followed by a plateau phase ($\Delta f_{plateau}$), within which no further significant Δf occurred. This trend in decreased Δf was suggestive of possible mass addition at the sensor surface and this was supported by fluorescence microscopy that demonstrated the presence of randomly distributed microspheres on the sensor surface at the conclusion of experiments (Fig. 1 inset).

The plateau phase in response to each injection indicates that no further mass addition is being registered at the sensor surface during the final 600 s of each experiment, which may be due to saturation of available binding sites, or that microspheres available for further binding have been eluted from the flow cell. Fig. 1 clearly indicates it is the latter as subsequent injections of microspheres do result in further $\Delta f_{binding}$ with the same crystal. The stability of this phase also suggests that a stable binding interaction has occurred between the microspheres and the sensor surface, as any subsequent microsphere detachment would have resulted in a positive Δf.

These experiments also served to determine the level of precision that could be attained using this novel experimental configuration and the extent of microsphere binding to the cell-free sensor surface *in situ*. The frequency responses for three individual crystals in response to each addition are shown in Table 1. The coefficient of variation for this data was 15.0%, which indicates the level of reproducibility that can be expected between crystals in response to a specific volume of microspheres. After each injection, a small transient frequency increase was observed at the start of each experiment. This transient alteration in the baseline occurs at a time point prior to which the microsphere suspension is estimated to arrive at the flow cell based on calculations of flow rate, tubing diameter and length.

Thus, despite the inclusion of the Rheodyne valve in this experimental system we postulate that the transient frequency change be attributed to pressure changes at the introduction of the microsphere suspension.

Table 1
Total frequency changes for a 10 MHz crystal with protein thin film to injections of 0.5 μm microspheres

	Injection 1	Injection 2	Injection 3	Injection 4	Injection 5	Injection 6	Mean	S.D.
Δ time (s)	1800	1800	1800	1800	1800	1800	1800	
Δ Frequency (Hz)								
Crystal 1	−97.44	−142.28	−286.40	−190.86	−183.37	−171.94	−178.72	57.3
Crystal 2	−193.04	−183.36	−170.49	−191.01	−126.11	−149.09	−168.85	24.2
Crystal 3	−129.88	−134.50	−121.82	−148.13	−116.58	−94.98	−124.32	16.5

3.2. Biosensor/microsphere interaction assay

Exposure of cell-coated biosensors to microspheres yielded a considerably more complex response to that seen in the absence of the cells (Fig. 2). Arrival of the microspheres at the biosensor surface initially resulted in a positive frequency response ($\Delta f_{positive}$) following each injection reaching maxima, e.g. 35.49, 46.96 and 60.98 Hz respectively. After reaching a maximum following each injection (at 285, 468 and 500 s respectively) a significant frequency decrease then occurs [−50.06 Hz (810 s), −38.89 Hz (1106 s) and −28.59 Hz (1200 s)] following a similar pattern to that observed during $\Delta f_{binding}$ with cell-free sensors.

The total frequency response in each case again followed a trend that might imply added mass at the sensor surface. It is important to note that negative frequency responses have been attributed to a number of other phenomena occurring at the sensor substrate interface for example, Cans et al. (2001) found negative Δfs using their biosensor in response to temperature and pressure changes during solution exchange. In this study we excluded the generation of these artefacts by using temperature-equilibrated microsphere-suspensions and a Rheodyne™ injection port with a make before break valve that prevents pressure changes being introduced to the flowing mobile phase upon solution exchange. As changes in the viscosity and density of the liquid above the crystal surface can also induce significant frequency shifts (Kanazawa and Gordon, 1985) maintaining these solution based parameters throughout experiments ensured such factors did not contribute to the observed frequency responses. Examination of biosensors at the conclusion of experiments using fluorescence microscopy confirmed the presence of microspheres on the sensor surface (inset Fig. 2) and therefore that the net negative Δf obtained for each injection can be attributed, in part, to mass addition at the sensor surface.

Positive frequency responses have been reported previously using cellular biosensors as a consequence of stimulated vesicle exocytosis after cell membrane stimulation (Cans et al., 2001), as a response to cytosolic viscosity changes mediated by alterations in cytoskeletal rigidity (Marxer et al., 2003a) and as a result of non-proteolytic induced cell-detachment from the sensor surface (Marx et al., 2005). In this study the Hoechst/PI assay confirmed that $\Delta f_{positive}$ could not be attributed to cell-detachment from the sensor during experiments as no significant difference in cell number (viable, apoptotic or necrotic) between cells exposed to microspheres *in situ* in the QCM flow cell and matched biosensor controls in culture were observed (see Fig. 3). These results also confirm that quartz sensor shear-oscillation and serum-depletion of the media mobile phase are not detrimental to the cells during experiments, which have been identified as fundamental parameters in this type of experiment (Edvardsson et al., 2005; Simm et al., 1997). Osmolaric effects can also be excluded as a possible cause for $\Delta f_{positive}$ as both the mobile phase and the media-suspended microspheres had similar osmolarities when measured using depression point freezing (305:310 mOsmol/kg respectively). As $\Delta f_{positive}$ is not observed with cell-free sensors investigated using the same experimental design, cell-membrane stimulation and cytoskeletal alterations seem potential candidates for the frequency upshift.

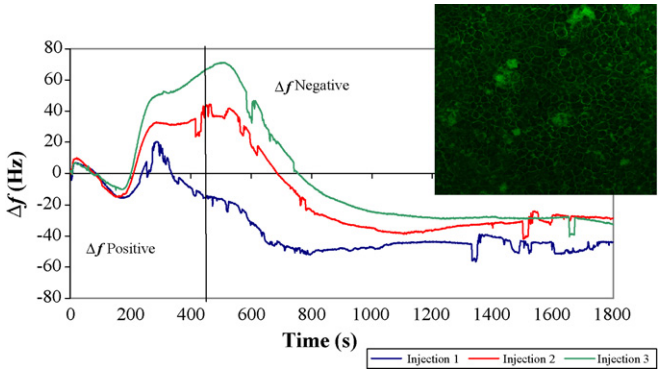

Fig. 2. Representative trace demonstrating the frequency response of a cell-coated crystal to three injections of microsphere suspension. Inset: representative photomicrograph of the H376 cell-coated sensor surface after exposure to the microspheres (Magnification× 200).

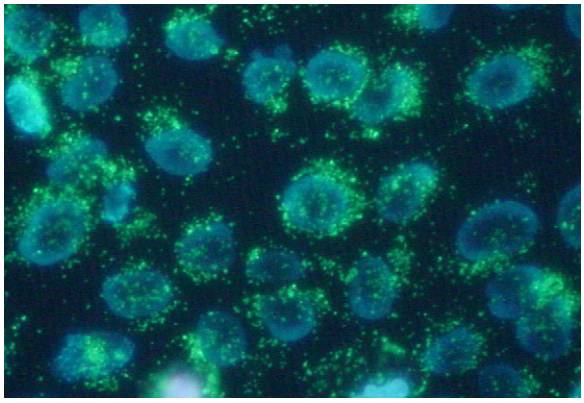

Fig. 3. H376 cells stained with the vital dyes Hoechst 33342 and propidium iodide after incubation with microspheres *in situ* in the QCM flow cell (Magnification× 320).

Importantly positive frequency shifts have also been observed when the stiffness of epithelial cells attached to quartz crystals increases, as indicated by concomitant changes in oscillation amplitude and transient delay time constant (Marxer et al., 2003b). The contribution of cytoskeletal intermediate filaments to cell stiffening is well recognised (Wang and Stamenovic, 2000) and can be affected by cytoskeletal-linked, receptor activation which significantly affects geometric changes in the cytoskeleton (Huang et al., 2005). Disruption of the actin microfilament system (one of the three microfilament systems responsible for cytoskeletal architecture) of bovine endothelial cells has also been shown to directly affect frequency response when studied *in situ* on a QCM (Marx et al., 2001). These authors suggested that the reported frequency decrease was due to increased cell rounding and 'a less-spread morphology' resulting in decreased interaction of the cell-basolateral membrane with the sensor surface. Mammalian cell cytoskeletons are responsible for maintaining cell shape, and dynamic cellular processes such as cell migration and endocytosis via active remodelling of the motor proteins responsible (Möller et al., 2002). These studies highlight the role of cytoskeletal alteration in mediating frequency responses when cells are incorporated as part of the system sensing design. It is therefore possible that cell membrane stimulation and/or cytoskeletal alteration induced by microsphere binding may result in the $\Delta f_{positive}$ observed in this study.

To further investigate the H376 cell response to microsphere interactions SEM studies were performed. These revealed close association of microspheres with cell peripheries (Fig. 4) and the apical membrane surface, but more importantly some microspheres of less defined outline consistent with their positioning in a different focal plane (Fig. 5). The proximity of these 'unfocussed' microspheres to the focussed, combined with the uniformly focussed underlying substrate indicates the possibility that some microspheres are located beneath the plasma membrane. Uptake of polystyrene microspheres by epithelial cells has been reported previously (Innes and Ogden, 1999; Hall et al., 2000; Zauner et al., 2001), and although not a commonly ascribed function for such cell types may reflect their innate

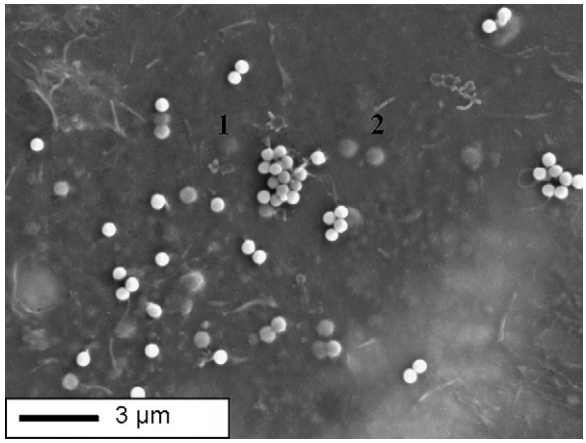

Fig. 5. SEM micrographs of confluent monolayers of H376 cells after incubation with 0.5 μm microspheres that illustrate binding to the apical cell membrane (1) and those that are occluded by the cell membrane (2) Magnification× 6000.

ability to internalise material from the interstitial environment. Cross sectional TEM analysis confirmed that the H376 cells were internalising the microspheres (Fig. 6). Examination of ultrathin sections of H376 cells after microsphere exposure for 1 h at 37 °C demonstrated the presence of numerous intracellular microspheres (some with evidence of vesicular membranes) in all the cells examined providing clear evidence that some internalisation process had occurred as a result of membrane stimulation by the microspheres. This was also indicated by altered surface topography which showed increased membrane 'ruffling' with timed incubations of microsphere–cell monolayer interactions studied using TEM revealing that this uptake process was initiated at 10 min and maintained until the conclusion of experiments.

Internalisation of the microspheres indicates that active cytoskeletal re-modelling must occur during the time-course of the QCM experiments as these processes are well documented in the role they play in cellular uptake (Swanson and Watts, 1995; Da Costa et al., 2003; Eitzen, 2003; Nabi and Le, 2003). This also supports findings by Steinem et al., 1997; Cans et al.,

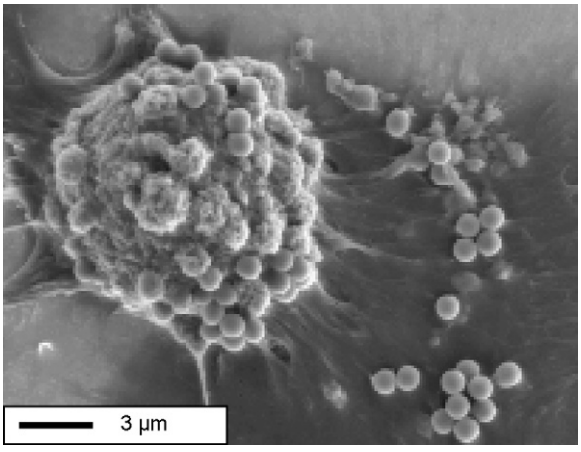

Fig. 4. Single H376 cell with surface bound polystyrene microspheres (Magnification× 5,500).

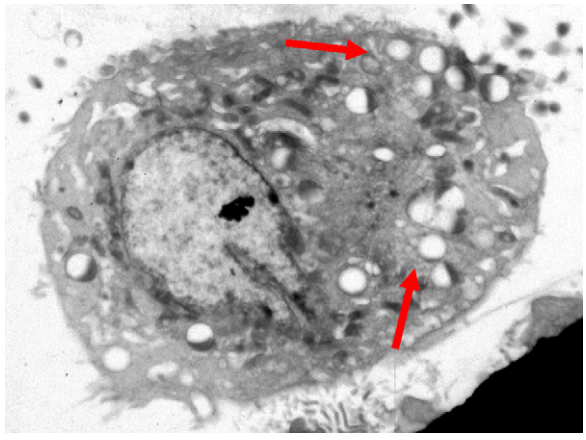

Fig. 6. TEM micrograph of a single H376 cell after incubation with microspheres for 1 h prior to fixation (Magnification× 2750).

2001; Marx et al., 2001; Marxer et al., 2003b and adds weight to the postulation that altered cellular rigidity through remodelling of the H376 cytoskeleton gives rise to the unique frequency responses reported here.

As the use of inhibitors to arrest epithelial and endothelial cytoskeletons *in situ* on a QCM have themselves been shown to induce frequency shifts (Steinem et al., 1997; Marx et al., 2001) it was impossible to investigate the response of the H376 cells to microspheres after inhibition of their uptake machinery *in situ*. However, static experiments of H376 cell–microsphere interactions after cytochalasin treatment (unpublished data) using TEM demonstrate an absence of microsphere uptake in the presence of actin disruption which further supports the hypothesis that cytoskeletal alterations and cellular uptake by the H376 cells is responsible for the unique frequency response observed in this study.

4. Conclusions

This study highlights the ability of the QCM technique to follow the responses of viable human oral epithelial cells to microspheres in a dynamic and non-invasive way. The frequency profiles recorded indicate a general response from a population of cells which in conjunction with microscopic evidence highlights the ability of the technique to follow mass addition to the biosensor as indicated by the reduction in frequency baseline at the end of each experiment in real-time. Furthermore the sensitivity of this technique allows insight into the complex responsiveness of the cells to changes in their environment as evidenced by the unique frequency profiles generated here. It also offers significant advantages in that it can be used to follow cell responses under conditions of fluid flow, as would occur in the oral cavity. Equally it could be applied to investigate interactions of microparticles with a variety of surface modifications to generate optimal response profiles and thus potentially applied to high throughput screening. Future work to de-convolute the responses obtained and investigate the effect of dissipative forces during such interactions is imperative as the ability of the technique to follow endocytic processes would be especially valuable to a wide range of fields in cell biology and as such could also be applied to basic cell-research studies.

Acknowledgements

This work was carried out as part of an EPSRC-Case award (99/803153) for JE funded in collaboration with GlaxoSmithKline R&D. The H376 cell line was kindly donated by Professor Stephen Prime of the Department of Oral Medicine, Pathology and Microbiology, University of Bristol.

Appendix A. Supplementary data

Supplementary data associated with this article can be found, in the online version, at doi:10.1016/j.bios.2007.11.020.

References

Aizawa, H., Kurosawa, S., Tanaka, M., Wakida, S., Talib, Z.A., Park, J.W., Yoshimoto, M., Muratsugu, M., Hilborn, J., Miyake, J., Tanaka, H., 2001. Mater. Sci. Eng. C 17, 127–132.
Cans, A.-S., Höök, F., Shupliakov, O., Ewing, A.G., Eriksson, P.S., Brodin, L., Orwar, O., 2001. Anal Chem. 73, 5805–5811.
Cavic, B.A., Freedman, J., Morel, Z., Mody, M., Rand, M.L., Stone, D.C., Thompson, M., 2001. Analyst 126, 342–348.
Chickering, D.E., Mathiowitz, E., 1995. J. Control. Rel. 34, 251–262.
Da Costa, S.R., Okamoto, C.T., Hamm-Alvarez, S.F., 2003. Adv. Drug Deliv. Rev. 55, 1359–1383.
Doucet, O., Robert, C., Zastrow, L., 1996. Toxicol. in vitro 10, 305–313.
Edvardsson, M., Rodahl, M., Kasemo, B., Höök, F., 2005. Anal. Chem. 77, 4918–4926.
Eitzen, G., 2003. Biochim. Biophys. Acta 1641, 175–181.
Farokhzad, O.C., Khademhosseini, A., Jon, S., Hermmann, A., Cheng, J., Chin, C., Kiselyuk, A., Teply, B., Eng, G., Langer, R., 2005. Anal. Chem. 77, 5453–5459.
Fredriksson, C., Khilman, S., Kasemo, B., Steel, D.M., 1998a. J. Mater. Sci. Mater. Med. 9, 785–788.
Fredriksson, C., Khilman, S., Rodahl, M., Kasemo, B., 1998b. Langmuir 14, 248–251.
Furtado, L.M., Thompson, M., 1998. Analyst 123, 1937–1945.
Gryte, D.M., Ward, M.D., Hu, W.S., 1993. Biotechnol. Prog. 9, 105–108.
Hall, W., Ogden, G.R., Saleh, A.H., Hopwood, D., Ross, P.E., 2000. J. Oral Pathol. Med. 29, 220–225.
Höök, F., Rodahl, M., Brzezinski, P., Kasemo, B., 1998. Langmuir 14, 729–734.
Huang, H., Sylvan, J., Jonas, M., Barresi, R., So, P.T.C., Campbell, K.P., Lee, R.T., 2005. Am. J. Physiol. Cell Physiol. 288, C72–C80.
Innes, N.P.T., Ogden, G.R., 1999. Arch. Oral Biol. 44, 519–523.
Janshoff, A., Wegener, J., Sieber, M., Galla, H.J., 1996. Eur. Biophys. J. 25, 93–103.
Janshoff, A., Steinem, C., Sieber, M., El Bayâ, M.A., Schmidt, A., Galla, H.-J., 1997. Eur. Biophys. J. 26, 261–270.
Kanazawa, K.K., Gordon, J.G., 1985. Anal. Chim. Acta 175, 99–105.
Kockisch, S., Rees, G.D., Young, S.A., Tsibouklis, J., Smart, J.D., 2001. J Control. Release 77, 1–6.
Kockisch, S., Rees, G.D., Young, S.A., Tsibouklis, J., Smart, J.D., 2003. Pharm. Sci. 92, 1614–1623.
Lawrence, J.N., Starkey, S., Dickson, F.M., Benford, D.J., 1996. Toxicol. in vitro 10, 331–340.
Lord, M.S., Modin, C., Foss, M., Duch, M., Simmons, A., Pedersen, F.S., Milthorpe, B.K., Besenbacher, F., 2006. Biomaterials 27, 4529–4537.
Marx, K.A., Zhou, T., Montrone, A., Schulze, H., Braunhut, S.J., 2001. Biosens. Bioelectron. 16, 773–782.
Marx, K.A., Zhou, T., Warren, M., Braunhut, S.J., 2003. Biotechnol. Prog. 19, 987–999.
Marx, K.A., Zhou, T., Montrone, A., McIntosh, D., Braunhut, 2005. Anal. Biochem. 343, 23–34.
Marxer, C.G., Coen, M.C., Greber, T., Greber, U.F., Schlapbach, L., 2003a. Anal. Bioanal. Chem. 377, 578–586.
Marxer, C.G., Coen, M.C., Bissig, H., Greber, U.F., Schlapbach, L., 2003b. Anal. Biochem. Chem. 377, 570–577.
Matsuda, T., Kishida, A., Ebato, H., Okahata, Y., 1992. ASAIO J. 38, M171–M173.
Möller, W., Hofer, T., Ziesenis, A., Karg, E., Heyder, J., 2002. Toxicol. Appl. Pharmacol. 182, 197–207.
Nabi, I.R., Le, P.U., 2003. J. Cell Biol. 161 (4), 673–677.
Nimeri, G., Fredriksson, C., Elwing, H., Liu, L., Rodahl, M., Kasemo, B., 1998. Colloids Surf. B 11, 255–264.
Norton, L.A., Andersen, K.L., Arenholt-Bindslev, D., Andersen, L., Melsen, B., 1995. Arch. Oral Biol. 40, 863–872.
Paul, F., Pavey, K.D., Payne, R., 2001. Int. Pat., WO 00/25118.
Pavey, K.D., Hunter, A.C., Paul, F., 2003. Biosens. Bioelectron. 18, 1349–1354.
Prime, S.S., Nixon, S.V.R., Crane, I.J., Stone, A., Matthews, J.B., Maitland, N.J., Remnant, L., Powell, S.K., Game, S.C., Scully, C., 1990. J. Pathol. 160, 259–269.

Redepenning, J., Schlesinger, T.K., Mechalke, E.J., Puleo, D.A., Bizios, R., 1993. Anal. Chem. 65, 3378–3381.
Reipa, V., Almeida, J., Cole, K.D., 2006. J. Micro. Methods 66, 449–459.
Sauerbrey, G., 1959. Z. Physik. 155, 206–222.
Simm, A., Bertsch, G., Frank, H., Zimmerman, U., Hoppe, J., 1997. J. Cell Sci. 110, 819–828.
Steinem, C., Janshoff, A., Wegener, J., Ulrich, W., Willenbrink, W., Sieber, M., Galla, H., 1997. Biosens. Bioelectron. 12, 787–808.
Swanson, J.A., Watts, C., 1995. Trends Cell Biol. 5, 424–428.
Wang, N., Stamenovic, D., 2000. Am. J. Physiol. Cell Physiol. 279, C188–C194.
Wegener, J., Janshoff, A., Galla, H.J., 1998. Eur. Biophys. J. 28, 26–37.
Wegener, J., Seebach, J., Janshoff, A., Galla, H.-J., 2000. Biophys. J. 78, 2821–2833.
Wegener, J., Janshoff, A., Steinem, C., 2001. Cell Biochem. Biophys. 34, 121–151.
Zauner, W., Farrow, N.A., Haines, A.M.R., 2001. J. Control. Release 71, 39–51.
Zhou, T., Marx, K.A., Warren, M., Schulze, H., Braunhut, S.J., 2000. Biotechnol. Prog. 16, 268–277.